

## Electronic Properties of Carbon Nanotubes with Covalent Sidewall Functionalization

Jijun Zhao,<sup>\*,†</sup> Hyoungki Park,<sup>†</sup> Jie Han,<sup>‡</sup> and Jian Ping Lu<sup>\*,†</sup>

Department of Physics and Astronomy, University of North Carolina at Chapel Hill,  
Chapel Hill, North Carolina 27599, and Elore Corporation, NASA Ames Research Center,  
MS 229-1, Moffett Field, California 95051

Received: September 19, 2003

We show that covalent sidewall functionalization of single-wall nanotubes leads to drastic changes of nanotube electronic states near the Fermi level. The  $sp^3$  hybridization between the functional group and nanotube induces an impurity state near the Fermi level. The impurity state is found to be extended over a large distance ( $>1$  nm) even though the structural deformation is confined to the vicinity of the functionalizing site. Thus, dramatic changes in the conductive properties of the nanotube can be expected even if the concentration of functionalization molecules is small. This effect provides an effective pathway for band structure engineering, nanoelectronic device, and sensor applications through covalent sidewall functionalization.

In recent years, carbon nanotubes have attracted considerable attention due to their unique structural, mechanical, and electronic properties. Chemical functionalization of carbon nanotubes might lead to new opportunities in nanotube-based materials and devices.<sup>1</sup> Experiments on nanotube functionalization start from the fluorination of single-walled nanotubes (SWNTs)<sup>2</sup> and the substitution reaction of fluorinated SWNTs in solutions.<sup>3–5</sup> Direct functionalization to the sidewall of SWNTs by various chemical groups such as atomic hydrogen,<sup>6–8</sup> nitrene,<sup>9</sup> aryl groups,<sup>10,11</sup> nitrenes, carbenes, radicals,<sup>12</sup> COOH, NH<sub>2</sub>,<sup>13</sup> 1,3-dipolar cycloadditions,<sup>14</sup> *N*-alkylidene amino groups,<sup>15</sup> alkyl groups,<sup>16</sup> and aniline<sup>17</sup> has also been reported. In general, changes in physical properties of carbon nanotubes upon functionalization are found. For instance, the band-to-band transition feature of  $\pi$  electrons in the UV–vis spectra of pristine SWNTs is disrupted by covalent functionalization.<sup>4,10,15–17</sup> The resistance of functionalized SWNTs dramatically changes with respect to the pristine samples.<sup>2,4,8,18</sup> Shifting of Raman spectra shows evidence of charge transfer from the functional groups to SWNTs.<sup>13</sup>

Theoretically, little is known about the effect of covalent sidewall functionalization on electronic structures of carbon nanotubes. From previous works, it was shown that the electronic and transport properties of SWNTs can be significantly modified upon adsorption of selective gas molecules (NO<sub>2</sub>, O<sub>2</sub>)<sup>19–22</sup> or noncovalent functionalization of aromatic organic molecules.<sup>23,24</sup> The effect of substitutionally doped impurities on the conductance of SWNTs was studied by Choi et al.<sup>25</sup> and Guo's group.<sup>26</sup> Andriotis et al. studied the conductance and HOMO–LUMO gap for nanotubes with atomic hydrogen adsorption.<sup>27</sup> In this letter, we present *ab initio* results on the electronic properties of covalent sidewall functionalized SWNTs. The carboxylic acid group (COOH) is used as the main prototype for functionalization, while other groups such as H, NH<sub>2</sub>, CH<sub>3</sub>, OH, and F are also studied.

Density-functional calculations are performed using plane-wave pseudopotential methods<sup>28,29</sup> within the generalized gradi-

ent approximation (GGA).<sup>30</sup> Ultrasoft pseudopotential<sup>31</sup> is used to model the ion–electron interaction. The cutoff energy for the plane-wave basis is chosen as 300 eV, while further increasing the cutoff shows little difference on the results. A one-dimensional periodic boundary condition is applied along tube axis. A  $\Gamma$  point is used for geometry optimizations with 0.01 eV/Å converge tolerance of force on each atom. Ten uniform  $\mathbf{k}$  points are used for sampling the one-dimensional Brillouin zone of nanotube in the self-consistent band-structure calculations, after which non-self-consistent calculations with 30  $\mathbf{k}$  points are performed to generate the fine band structures. To study the effect by individual functional group, we include one functional molecule in two unit cells of the zigzag tube (supercell length  $a = 8.52$  Å) or three unit cells of the armchair tubes ( $a = 7.38$  Å) in a typical computational supercell.

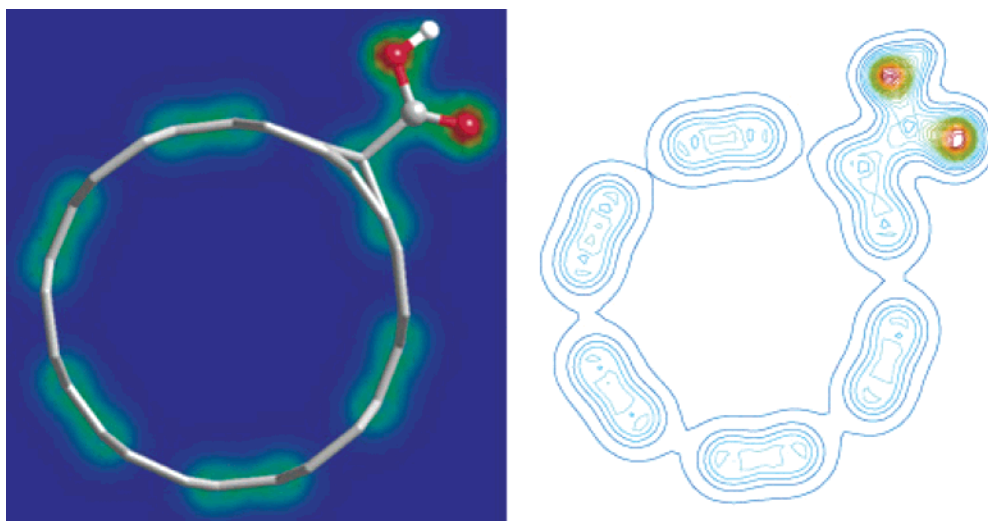
As shown in Figure 1, the COOH group induces a local distortion along the radial direction on the tube sidewall, which can be understood by the local  $sp^3$  rehybridization of C–C bonding. The overlap of valence electron density, shown in Figure 1 as a contour plot, indicates the formation of a covalent bond between the functional group and the nanotube. The same behaviors are found for all the functional groups studied and can be considered as the common features of the covalent sidewall functionalization of carbon nanotubes.

Table 1 summarizes the binding energy<sup>32</sup> and C–C bond length between the COOH group and the carbon nanotubes of different size and chirality. In all the systems studied, the C–C bond length between the C atom on the tube and that of the molecule is around 1.54 Å, while those of the C atom and its three nearest neighbors on the nanotube are around 1.51 Å, both of which are close to the C–C distance in the  $sp^3$ -hybridized diamond phase and significantly larger than the C–C bond length of 1.42 Å in the perfect nanotube with  $sp^2$  hybridization. The C–C bond lengths in the nanotube beyond the first neighbors are found to be little affected by the functionalization. Our results clearly demonstrate the presence of a local  $sp^3$  defect on the tube sidewall due to the tube–molecule covalent bonding. Table 1 shows that the binding energy between the COOH group and the SWNTs is insensitive to tube size and chirality. This can be understood by the localized nature of the  $sp^3$  rehybrid-

\* Authors to whom correspondence may be addressed. E-mail: zhaojj@mail.unc.edu (J.Z.); jpl@physics.unc.edu (J.P.L.).

<sup>†</sup> University of North Carolina.

<sup>‡</sup> Elore Corporation.



**Figure 1.** Atomic structure (left) of COOH-attached (6,6) SWNT and contour plot of electron density (right) on the slice passing through the COOH group. Red, yellow, green, and blue colors on the contour plot indicate electron density from higher density to lower density. The structural distortion on the nanotube is found to confine to the nearest neighbors of the bonding site.

**TABLE 1: Binding Energy  $E_b$  (eV)<sup>32</sup> and C–C Bond Length  $d$  (Å) between Different Carbon Nanotubes and COOH Group**

	(5,5)	(6,6)	(7,7)	(9,0)	(10,0)	(11,0)
$E_b$ (eV)	1.76	1.78	1.79	1.42	1.42	1.55
$d$ (Å)	1.537	1.543	1.547	1.541	1.547	1.549

ization and structural distortion. The small systematic difference between zigzag and armchair tubes can be attributed to small differences in the optimal local bonding configurations. For armchair tubes, the COOH group is perpendicularly attached to the tube sidewall, while for the zigzag tube, the molecule is slightly slanted. For the other functional groups studied, including  $\text{NH}_2$ ,  $\text{CH}_3$ , H, and OH, the calculated binding energies vary between 1.5 and 2.5 eV, indicating the strength of the covalent bonding depends on the functionalizing molecule, as expected.

In contrast to the tightly localized nature of structural deformation, we found that all functionalization configurations universally induce an impurity state intrinsic to the nanotube with impurity wave function extended over a relatively large distance. On the basis of the optimized geometries, we systematically investigated the electronic band structures of both metallic and semiconducting SWNTs functionalized with different functional groups (COOH,  $\text{CH}_3$ ,  $\text{NH}_2$ , H, OH, F, etc.). As representatives, the band structures of the armchair metallic (6,6) tube functionalized by COOH and  $\text{NH}_2$  groups are shown in Figure 2. In Figure 3, we compare the covalent functionalization by atomic hydrogen to the substitutional doping by nitrogen atom for a semiconducting (10,0) tube. For all the functional groups considered, an individual functionalization-induced  $\text{sp}^3$  defect on the tube sidewall induces a half-occupied impurity state around the Fermi level. Including more functional groups in the computational supercell will lead to multiple impurity states around the Fermi level. The appearance of a half-filled level in the gap was also found in a recent ab initio study of silicon-doped SWNTs with chemical binding of atoms (F, Cl, H) and molecules ( $\text{CH}_3$ ,  $\text{SiH}_3$ ) at silicon substitutional sites.<sup>33</sup>

In the cases of metallic nanotubes, we find that the original  $\pi$ – $\pi^*$  band crossing of either the armchair (6, 6) or the zigzag (9, 0) tube is disturbed by the sidewall functionalization (see Figure 2). A band gap opens up between the conduction and valence bands. This effect can be understood by the breaking

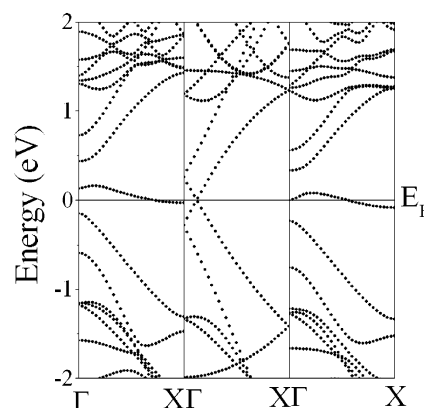


**Figure 2.** Band structure of the pristine (middle), COOH-attached (left), and  $\text{NH}_2$ -attached (right) armchair (6,6) SWNT. One functional group is included per three unit cells of the tube. The  $\text{sp}^3$  defect-induced impurity state at the Fermi level is clearly seen in both cases.

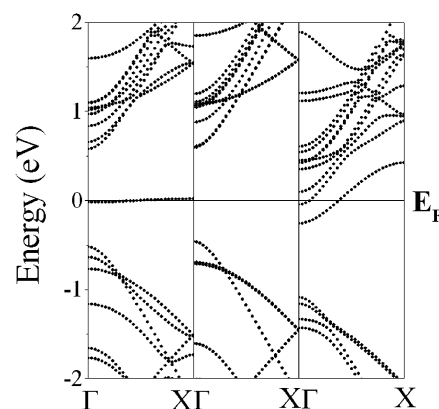


**Figure 3.** Band structure of the pristine (middle), hydrogen-functionalized (left), and substitutional nitrogen-doped (right) zigzag (10,0) SWNT. One H or N atom is included per two unit cells of the tube. There is no induced impurity state near the Fermi level in the case of substitutional doping.

of nanotube mirror symmetry<sup>34</sup> due to strong tube–molecule interaction, similar to previous results of the Ti chain interacting with metallic nanotubes.<sup>35</sup> Compared to those of pristine tubes, the band structures for either the valence or conduction bands are not significantly changed by the functionalization. The band

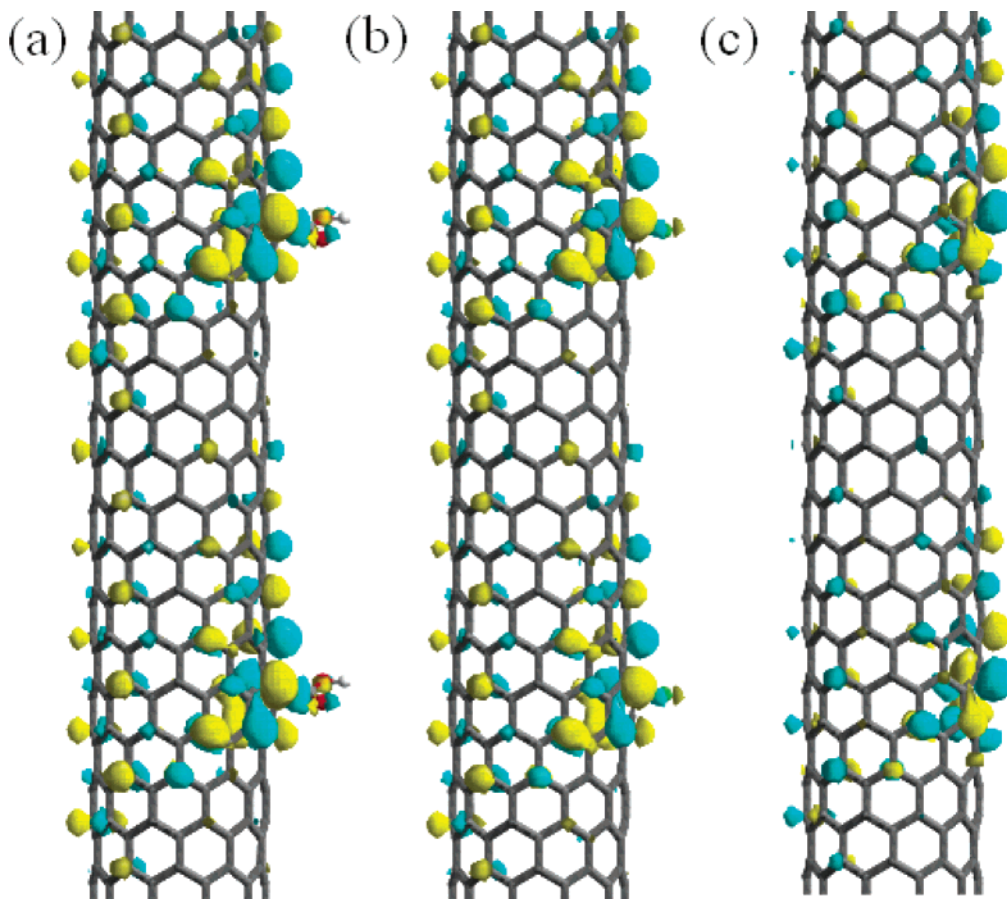


**Figure 4.** Isosurface plot of the impurity state wave function at the Fermi level (two colors represent  $\pm$ polarity of the wave function). (a) COOH-functionalized (10,0) SWNT; (b) F-functionalized (10,0) SWNT; (c) (10,0) SWNT with a C vacancy on the sidewall. In contrast to the structural modification, the impurity state is distributed over a large area of nanotube sidewall. The similarities of three cases are striking. The supercells used for all three calculations include one molecule/vacancy per five unit cells of the zigzag tube ( $a = 21.3$  Å).

degeneracy in the pristine SWNT is partially removed by the perturbation from the functional group.

We found that the effect of modification on electronic properties of nanotubes is independent of the choice of functional group. Systematical studies on different functional molecules (COOH,  $\text{NH}_2$ , OH,  $\text{CH}_3$ , H, F) show similar results. Shown in Figure 4 is the wave function associated with induced impurity state. This electronic state is found to extend over a much larger space ( $>10$  Å) than that of the structural deformation around the functionalization site ( $<5$  Å). The impurity state will act as a strong scattering center for the conduction carriers around the Fermi level and thus significantly affect the ballistic transport of metallic nanotubes. This is consistent with recent experimental observations.<sup>2,4</sup>

The effects of functionalization on semiconducting nanotubes are similar to those of the metallic tubes. To understand the particular influence of the  $\text{sp}^3$  defect due to tube–molecule covalent interaction, we exploit the difference between the covalent functionalization and substitutional doping on the tube sidewall. Figure 3 shows the band structures of the (10,0) tube both by substitutional nitrogen doping and by atomic hydrogen functionalization. The number of electrons in the supercell is the same in both systems. As in the case of metallic tube, the hybridization between the functional group and the nanotube introduces an impurity state in the middle of the gap region for the pristine semiconducting (10,0) tube. On the contrary, we find that band structures near the Fermi level are not significantly changed by the substitutional nitrogen doping. The extra valence electrons from the nitrogen dopant occupy the nanotube

conduction band and shift the Fermi level toward the conduction band, instead of forming an additional impurity state. Our results on substitutional nitrogen-doped nanotubes agree well with the previous experimental and theoretical studies.<sup>36</sup> The remarkable difference between covalent functionalization and substitutional doping can be understood by the fact that substitutional doping by nitrogen does not disturb the  $\text{sp}^2$  hybridization of nanotube  $\pi$  electrons.<sup>37</sup> It is worthy to point out that the effect of covalent functionalization is also different from alkali metal doping. In the alkali-metal-intercalated nanotubes, electrons from alkali metal atoms completely transfer to the nanotube and occupy the nanotube conduction bands.<sup>38</sup> Therefore the covalent sidewall functionalization may provide a unique and feasible way of controlling the electronic properties of the carbon nanotube that are different from either substitutional doping or metal intercalation.

Moreover, it is also interesting to compare the covalent sidewall functionalization to the structural defects on the nanotube sidewall, such as pentagon–heptagon (5–7) pair<sup>39</sup> and vacancy.<sup>40</sup> Our calculations show that an individual vacancy can also induce an additional state around Fermi energy, whereas the 5–7 topological defect does not have such effect. This can be understood by the fact that the 5–7 topological defect does not alter the  $\text{sp}^2$  bonding nature of any C atom on the tube sidewall, while a vacancy defect will alter the  $\text{sp}^2$  bonding of three C atoms around the vacancy. The similarity between sidewall covalent functionalization and vacancy defect can be clearly seen from the electron wave function associate with the impurity state. Shown in Figure 4a is the wave function of the



impurity state of COOH functionalized (10,0) tube. It is well spread from the covalent site to a large area of sidewall. Similar spreads of the wave function for the impurity states are found for the nanotube functionalized by other groups (Figure 4b), and a simple vacancy defect (Figure 4c). These results clearly show that any modification of the C—C bonding structure away from the  $sp^2$  bonding configuration will induce an impurity state in the gap region and significantly change the electronic states and conducting properties of the carbon nanotube.

The results we found here are in sharp contrast to the noncovalent functionalization, where slight modification of band structures of SWNTs were found.<sup>21,22,24</sup> The modification of electronic band structures of SWNTs by covalent functionalization thus provides a clear pathway for controlling the electronic properties of the carbon nanotube, band structure engineering, electronic, and chemical sensor applications.

**Acknowledgment.** This work is supported by University Research Council of University of North Carolina at Chapel Hill, Office of Naval Research (Grant No. N00014-98-1-0597) and the NASA Ames Research Center. We are thankful for computational support from UNC—Chapel Hill Academic Technology and Network.

## References and Notes

- (1) For recent reviews, see: (a) Hirsch, A.; *Angew. Chem. Int. Ed.* **2002**, *41*, 1853. (b) Sun, Y. P.; Fu, K.; Lin, Y.; Huang, W. *Acc. Chem. Res.* **2002**, *35*, 1096. (c) Niyogi, S.; Hamon, A.; Hu, H.; Zhao, B.; Bhowmik, P.; Sen, R.; Itkis, M. E.; Haddon, R. C. *Acc. Chem. Res.* **2002**, *35*, 1096. (d) Bahr, J. L.; Tour, J. M. *J. Mater. Chem.* **2002**, *12*, 1952.
- (2) Mickelson, E. T.; Huffman, C. B.; Rinzler, A. G.; Smalley, R. E.; Hauge, R. H.; Margrave, J. L. *Chem. Phys. Lett.* **1998**, *296*, 188.
- (3) Mickelson, E. T.; Chiang, I. W.; Zimmerman, J. L.; Boul, P. J.; Lozano, J.; Liu, J.; Smalley, R. E.; Hauge, R. H.; Margrave, J. L. *J. Phys. Chem. B* **1999**, *103*, 4318.
- (4) Boul, P. J.; Liu, J.; Mickelson, E. T.; Huffman, C. B.; Ericson, L. M.; Chiang, I. W.; Smith, K. A.; Colbert, D. T.; Hauge, R. H.; Margrave, J. L.; Smalley, R. E. *Chem. Phys. Lett.* **1999**, *310*, 367.
- (5) Khabashesku, V. N.; Billups, W. E.; Margrave, J. L. *Acc. Chem. Res.* **2002**, *35*, 1087.
- (6) Pekker, S.; Salvétat, J. P.; Jakab, E.; Bonard, J. M.; Forro, L. *J. Phys. Chem. B* **2001**, *105*, 7938.
- (7) Khare, B. N.; Meyyappan, M.; Kralj, J.; Wilhite, P.; Sisay, M.; Imanaka, H.; Koehne, J.; Baushchlicher, C. W., Jr. *Appl. Phys. Lett.* **2002**, *81*, 5237. (b) Khare, B. N.; Meyyappan, M.; Cassell, A. M.; Nguyen, C. V.; Han, J. *Nano Lett.* **2002**, *2*, 73.
- (8) Kim, K. S.; Bae, D. J.; Kim, J. R.; Park, K. A.; Lim, S. C.; Kim, J. J.; Choi, W. B.; Park, C. Y.; Lee, Y. H. *Adv. Mater.* **2002**, *14*, 1818.
- (9) Bahr, J. L.; Yang, J.; Kosynkin, D. V.; Bronikowski, M. J.; Smalley, R. E.; Tour, J. M. *J. Am. Chem. Soc.* **2001**, *123*, 6536.
- (10) Bahr, J. L.; Tour, J. M. *Chem. Mater.* **2001**, *13*, 3823.
- (11) Chen, J.; Hamon, M. A.; Hu, H.; Chen, Y.; Mao, A. M.; Eklund, P. C.; Haddon, R. C. *Science* **1998**, *282*, 95.
- (12) Holzinger, M.; Vostrowsky, O.; Hirsch, A.; Hennrich, F.; Kappes, M.; Weiss, R.; Jellen, F. *Angew. Chem., Int. Ed.* **2001**, *40*, 4002.
- (13) Chiu, P. W.; Duesberg, G. S.; Weglikowska, W. D.; Roth, S. *Appl. Phys. Lett.* **2002**, *80*, 3811.
- (14) Georgakilas, V.; Kordotos, K.; Prato, M.; Guldi, D. M.; Holzinger, M.; Hirsch, A. *J. Am. Chem. Soc.* **2002**, *124*, 760. (b) Georgakilas, V.; Tagmatarchis, N.; Pantarotto, D.; Bianco, A.; Briand, J. P.; Prato, M.; *Chem. Commun.* **2002**, 3050.
- (15) Stevens, J. L.; Huang, A. Y.; Peng, H.; Chiang, I. W.; Khabashesku, V. N.; Margrave, J. L. *Nano Lett.* **2003**, *3*, 331.
- (16) Saini, R. K.; Chiang, I. W.; Peng, H.; Smalley, R. E.; Billups, W. E.; Hauge, R. H.; Margrave, J. L. *J. Am. Chem. Soc.* **2003**, *123*, 3617.
- (17) Dyke, C. A.; Tour, J. M. *J. Am. Chem. Soc.* **2003**, *125*, 1156.
- (18) An, K. H.; Heo, J. G.; Jeon, K. G.; Bae, D. J.; Jo, C.; Yang, C. W.; Park, C. Y.; Lee, Y. H.; Lee, Y. S.; Chung, Y. S. *Appl. Phys. Lett.* **2002**, *80*, 4235.
- (19) Kong, J.; Franklin, N. R.; Zhou, C.; Chapline, M. G.; Peng, S.; Cho, K.; Dai, H. *Science* **2000**, *287*, 622. (b) Collins, P. G.; Bradley, K.; Ishigami, M.; Zettl, A. *Science* **2000**, *287*, 1801.
- (20) Sumanasekera, G. U.; Adu, C. K. W.; Fang, S.; Eklund, P. C. *Phys. Rev. Lett.* **2000**, *85*, 1096.
- (21) Jhi, S. H.; Louie, S. G.; Cohen, M. L. *Phys. Rev. Lett.* **2000**, *85*, 1710.
- (22) Zhao, J. J.; Buldum, A.; Han, J.; Lu, J. P. *Nanotechnology* **2002**, *13*, 195.
- (23) Sumanasekera, G. U.; Pradhan, B. K.; Romero, H. E.; Adu, K. W.; Eklund, P. C. *Phys. Rev. Lett.* **2002**, *89*, 166801.
- (24) Zhao, J.; Lu, J. P.; Han, J.; Yang, C. K. *Appl. Phys. Lett.* **2003**, *82*, 3746.
- (25) Choi, H. J.; Ihm, J.; Louie, S. G.; Cohen, M. L. *Phys. Rev. Lett.* **2000**, *84*, 2917.
- (26) Kuan, C. C.; Larade, B.; Mehrez, H.; Taylor, J.; Guo, H. *Phys. Rev. B* **2002**, *65*, 205416.
- (27) Andriotis, A. N.; Menon, M.; Srivastava, D.; Froudakis, G. *Phys. Rev. B* **2001**, *64*, 193401.
- (28) Payne, M. C.; Teter, M. P.; Allen, D. C.; Arias, T. A.; Joannopoulos, J. D. *Rev. Mod. Phys.* **1992**, *64*, 1045.
- (29) CASTEP is a density functional theory package with a plane-wave pseudopotential method distributed by Accelrys Inc. Milman, V.; Winkler, B.; White, J. A.; Pickard, C. J.; Payne, M. C.; Akhmatkaya, E. V.; Nobes, R. H. *Int. J. Quantum Chem.* **2000**, *77*, 895.
- (30) Perdew, J. P.; Wang, Y. *Phys. Rev. B* **1992**, *45*, 13244.
- (31) Vanderbilt, D. *Phys. Rev. B* **1990**, *41*, 7892.
- (32) The binding energy of the functional molecule is defined by the total energy gained by functionalization at equilibrium geometry:  $E_b = E_{\text{tot}}(\text{tube} + \text{molecule}) - E_{\text{tot}}(\text{tube}) - E_{\text{tot}}(\text{molecule})$ .
- (33) Fagan, S. B.; da Silva, A. J. R.; Mota, R.; Baierle, R. J. *Phys. Rev. B* **2003**, *67*, 033405.
- (34) Delaney, P.; Choi, H. J.; Ihm, J.; Louie, S. G.; Cohen, M. L. *Nature* **1998**, *391*, 466. (b) Delaney, P.; Choi, H. J.; Ihm, J.; Louie, S. G.; Cohen, M. L. *Phys. Rev. B* **1999**, *60*, 7899.
- (35) Yang, C. K.; Zhao, J. J.; Lu, J. P. *Phys. Rev. B* **2002**, *66*, 041403.
- (36) Czerw, R.; Terrones, M.; Charlier, J. C.; Blase, X.; Foley, B.; Kamalakaran, R.; Grobert, N.; Terrones, H.; Tekleab, D.; Ajayan, P. M.; Blau, W.; Ruhle, M.; Carroll, D. L. *Nano Lett.* **2001**, *1*, 457. (b) Terrones, M.; Ajayan, P. M.; Banhart, F.; Blase, X.; Carroll, D. L.; Charlier, J. C.; Czerw, R.; Foley, B.; Grobert, N.; Kamalakaran, R.; Redlich, P. K.; Ruhle, M.; Seeger, T.; Terrones, H. *Appl. Phys. A* **2002**, *74*, 355.
- (37) Yi, J. Y.; Bernholc, J. *Phys. Rev. B* **1993**, *47*, 1708.
- (38) Zhao, J. J.; Buldum, A.; Han, J.; Lu, J. P. *Phys. Rev. Lett.* **2000**, *85*, 1706. (b) Zhao, J. J.; Han, J.; Lu, J. P. *Phys. Rev. B* **2002**, *65*, 193401.
- (39) Charlier, J.; Ebbesen, T. W.; Lambin, Ph. *Phys. Rev. B* **1996**, *53*, 11108. (b) Pan, B. C.; Yang, W. S.; Yang, J. L. *Phys. Rev. B* **2000**, *62*, 12652.
- (40) Igami, M.; Nakanishi, T.; Ando, T. *J. Phys. Soc. Jpn.* **1999**, *68*, 716. (b) Igami, M.; Nakanishi, T.; Ando, T. *J. Phys. Soc. Jpn.* **2000**, *69*, 3146.